Georeferencing of Satellite Images with Geocoded Image Features

Yating Zhang [1], Heyi Li [2], Jing Yu [2], Pengjie Tao [1, 3, *]

[1] School of Remote Sensing and Information Engineering, Wuhan University, Wuhan 430079, China - yatingzhang@whu.edu.cn, pjtao@whu.edu.cn
[2] Institution of Remote Sensing Satellite, Chinese Academy of Space Technology, China - hey1li@126.com, yuj421@sina.com
[3] Hubei Luojia Laboratory, Wuhan 430079, China

Keywords: "Cloud Control" Photogrammetry, Geocoded image features, SIFT, Control points, Satellite image geometric positioning.

Abstract

Currently, using digital orthophoto map (DOM) and digital elevation model (DEM) as reference to achieve geometric positioning of newly acquired satellite images has become a popular photogrammetric approach. However, this method relies on DOM and DEM data which requires a lot of storage space in practical applications. In addition, for geometric positioning of satellite images, only sparse image feature points are needed as control points. Consequently, for the sake of convenience, the compression of control data emerges as a necessity with significant practical implications. This paper investigates a "cloud control" photogrammetry method based on geocoded image features. The method extracts SIFT feature points from DOMs, and obtains their ground coordinates, then constructs geocoded image feature library instead of DOM and DEM data as control, thus realizing the compression of control data. Experiments conducted on the Tianhui-1, Ziyuan-3 and Gaofen-2 satellite images demonstrate that the proposed method can achieve high-precision geometric positioning of satellite images and greatly reduce the size of the control data. Specifically, with the reduction of the reference data from 180~1248 MB 2 m DOM and 30 m DEM to 5~10 MB geocoded image features, the geopositional accuracies of the test Tianhui-1, Ziyuan-3 and Gaofen-2 images are improved from 3.12 pixels to 1.74 pixels, 3.69 pixels to 1.09 pixels, and 150.93 pixels to 2.67 pixels, respectively.

1. Introduction

In recent years, image acquisition technology has continuously developed, resulting in explosive growth of geospatial information data. Photogrammetry also follows the wave of the new round of scientific and technological revolution and has entered the stage of comprehensive intelligent sky-earth integrated photogrammetry (Zhang et al. 2021). To adapt to the characteristics of image data in this stage and meet the requirements of processing efficiency and high automation, the "cloud control" photogrammetry method (Zhang and Tao, 2017) was proposed, which regards generally accessed geo-encoded data as geometric control instead of field ground control points (GCPs). "Cloud control" photogrammetry no longer relies on field GCPs, but utilizes a wide range of ubiquitous geographic information data, including existing digital orthophoto maps (DOMs), digital elevation models (DEMs), digital line graphics (DLGs), light detection and ranging (LiDAR) points, images with known orientation parameters (Zhang et al., 2023), and even public geographic information data. A large amount of dense control points can be obtained through automatic matching, which alleviates the burden of obtaining control points by manual work in the field, reduces the acquisition time and manpower costs, and improves the processing efficiency.

Cloud control photogrammetry takes different forms depending on the geometric reference data used. The most commonly used form is based on DOM and DEM (Chen et al. 2017), which automatically extracts a large amount of control points from DOMs through image matching (Zhang et al. 2011). Currently, this form has gained wide applications in sensor geometric calibration and satellite image geometric positioning (Xie et al. 2021). Compared to the traditional in-orbit geometric calibration (Chen et al. 2015) and satellite image geometric positioning techniques using ground controls as reference, the cloud-control-based method offers advantages in terms of accuracy, cost, and timeliness (Cao et al. 2019). This method eliminates the need for ground geometric calibration fields and yield control points, reducing the burden of construction and maintenance. Additionally, positioning time and accuracy are no longer affected by the conditions of the calibration fields and control points. Tao et al. (2014) improved the internal accuracy of the ZY-1 02C satellite image from 6 to 8 pixels to sub-pixel level by using public geographic information data as reference data to realize the in-orbit geometric calibration. Zhang et al. (2016) proposed a method for orthorectification of optical satellite remote sensing images using SRTM-DEM as controls to improve the horizontal accuracies of the images. Zhong et al. (2019) used high-precision DOM and DEM as reference to obtain homonymous image points by matching between orthophotos, while the systematic error of rational function model (RFM) was compensated, thus realizing high-precision georeferencing of satellite images. Wang et al. (2021) used the SRTM as control to prevent convergence issues in the bundle adjustment caused by weak image intersection.

There has been extensive research on the DOM/DEM-based cloud control model for sensor geometric calibration (Zhang et al. 2019) and geometric positioning of satellite images (Cao et al. 2020). However, this method requires the acquisition and storage of DOMs and DEMs. Particularly in the global mapping with satellite images, storing worldwide DOM and DEM requires substantial disk storage space. Taking images with a resolution of 2 meters as an example, the volume of grayscale DOM data covering the global land reaches 42 TB; while the volume of 30 m DEM data also reaches 98GB. Addressing these shortcomings, this paper proposes a georeferencing method based on geocoded image features. Firstly, by extracting the scale-invariant feature transform (SIFT) feature points (Lowe, 2004) from DOMs and describing the features with SIFT vectors, the massive remote sensing image data is compressed into feature vectors as controls. Subsequently, the feature points are geocoded by obtaining their longitude and latitude coordinates from DOMs, and interpolating elevations from DEMs, respectively. All the geocoded SIFT

* Corresponding author

feature points are then organized and stored according to a certain data structure, constituting the image feature library. Finally, on this basis, the geocoded image feature library is used to match the features with the newly acquired image to provide dense digital control points. This paper addresses the challenge of storing, reading, and processing large amounts of data in "cloud control" photogrammetry that relies on DOMs and DEMs. By reducing the hardware requirements and improving processing efficiency, this approach enables "cloud control" photogrammetry that is less sensitive to control data.

2. Methodology

2.1 Image-Based "Cloud Control" Photogrammetry

Depending on the type of geometric reference data used, "cloud control" photogrammetry primarily manifests in the following forms: image-based cloud control, vector-based cloud control, cloud control based on LiDAR point clouds and digital line graphics (DLGs). Among these, the form based on DOM and DEM is the most commonly used. This method involves automatically extracting dense control points from DOM and DEM through image matching. To further reduce the dependence of "cloud control" photogrammetry on DOM and DEM, decrease data storage, and improve processing efficiency, this paper introduces a simple and small-volume generic feature to replace the massive volume of remote sensing images, exploring a method of cloud control photogrammetry based on a geocoded image feature database.

This method comprises three main parts: SIFT features extraction from DOMs, construction of the geocoded image feature database, and georeferencing satellite images based on the geocoded image feature database. The technical workflow is illustrated in Figure 1. The geographic coordinates (latitude, longitude, and elevation) of the extracted SIFT feature points are obtained based on the geoinformation of the DOM and DEM data. All the feature points extracted from the DOMs are reorganized according to their latitude and longitude coordinates and stored, completing the construction of the geocoded image feature database. By matching with these geocoded feature points, dense control points are obtained.

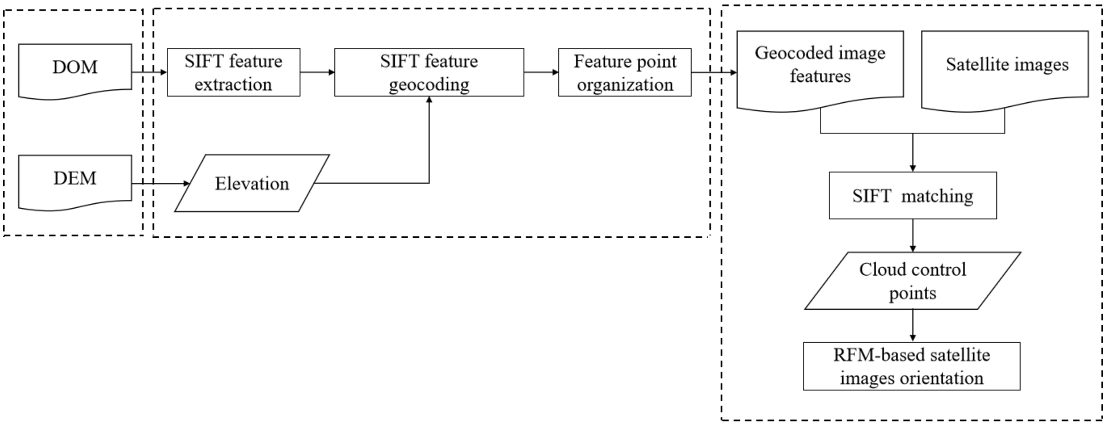

Figure 1. The workflow of the proposed georeferencing method for satellite images with geocoded image features.

2.2 Generation of Geocoded Image Features

To construct the image feature database, the first step is to extract SIFT features from the reference DOMs to obtain their feature and point coordinates. This involves sequentially reading each input DOM, extracting the position, scale, and orientation of each SIFT keypoint in the image, and creating a descriptor for each keypoint to generate a 128-dimensional SIFT feature vector. The extracted SIFT feature points from the images contain two important parts of information: the image coordinates of the feature points which represent their precise positions in the image, and the 128-dimensional feature vectors which describe the texture structure information within the neighborhood of the feature points in the image.

After obtaining the SIFT feature points from the reference DOMs, they are geocoded. Geocoding refers to the process of encoding a geographical location in order to obtain its precise position on the Earth's surface. Geocoding the SIFT feature points is done to give them a geographic attribute (including latitude, longitude, and elevation) alongside their SIFT feature vectors, thereby creating geocoded SIFT feature points. The specific implementation of geocoding for SIFT feature points is as follows:

a) Obtaining the latitude and longitude coordinates of the feature points from DOMs.
b) Interpolating the elevations of the feature point from DEMs.

Through the aforementioned steps, the geographic encoding of the feature points can be obtained. For a large amount of remote sensing images, these geocoded SIFT feature points form a dense control point cloud with image texture structure information, providing a data foundation for realizing cloud control photogrammetry.

2.3 Geocoded Image Feature Database

The geocoded image feature database is a repository that stores geocoded SIFT features, designed to enhance the efficiency of cloud control photogrammetry. By matching newly acquired images with the image features of reference DOMs stored in the database, it rapidly acquires the three-dimensional coordinates of corresponding ground points, forming a control point cloud. This process eliminates the need to extract features from each reference image individually, thereby accelerating the matching speed. The feature points stored in the database contain three-dimensional spatial information, allowing for the direct acquisition of their ground coordinates after matching, which optimizes the process. Moreover, as the database stores feature points instead of original images, it reduces the reliance on a large volume of reference image data and compresses the data size. Overall, the geocoded image feature database provides convenient data storage, management, and retrieval functions for "cloud control" photogrammetry.

Organizing geocoded feature points according to their map sheet for data arrangement forms the basis of constructing the geocoded image feature database. The establishment of this image feature database allows for the effective management and convenient extraction of feature information, facilitating the feature matching. Consequently, this enables the acquisition of dense control points on the images based on the three-dimensional coordinates of the matched feature points, thereby realizing "cloud control" photogrammetry. For the vast quantity of DOMs, the number of geocoded feature points required to be stored is substantial. Efficient organization of the geocoded image feature database can enhance storage, management, and query efficiency.

The construction of the geocoded image feature database involves the following steps:

a) Organize geocoded feature points according to standard map sheets. Depending on the resolution of the input DOMs, select appropriate longitude and latitude interval for segmentation.
b) Store the geocoded feature points in the database in a hierarchical tree structure, based on standard map sheets.

This indexing method not only improves query and retrieval efficiency but also allows effective management of the extensive control point information. Consequently, the geocoded image feature database should be organized as Figure 2.

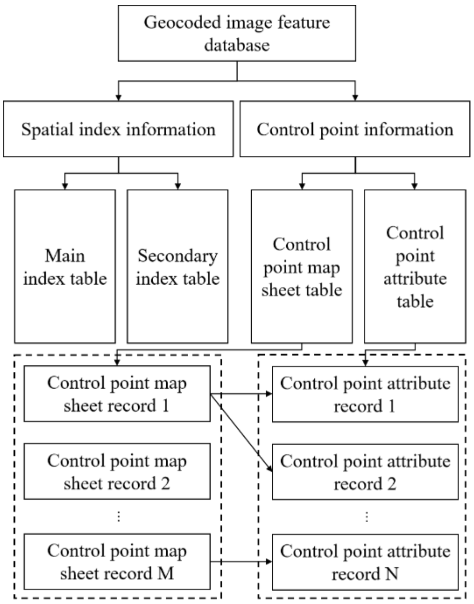

Figure 2. Structure of the geocoded image feature database.

The geocoded image feature database primarily contains two types of information: spatial index information and control point information. Through hierarchical indexing, all cloud control points within a region can be accurately extracted. Furthermore, for each cloud control point retrieved, its specific area can be determined based on its corresponding map sheet number and various levels of index information.

2.4 Retrieval of Cloud Control Points

Based on the constructed geocoded image feature database, newly acquired images are matched to acquire dense cloud control points, as illustrated in Figure 3. Using the geographic range information from the newly acquired satellite images, refer to the control point sheet to identify the corresponding sheet number. Subsequently, SIFT feature extraction is performed on the newly acquired images to obtain feature points. Based on the retrieved map sheet numbers, all control points contained within the corresponding map sheets in the control point attribute table are extracted. Each point is then individually assessed to determine whether it lies within the geographic range of the newly acquired image, including its expanded area.

Due to potential geographic inaccuracies in newly acquired satellite images, it is necessary to expand the geographical range of these images to match as many control points as possible. This expansion involves extending the geographic range of the newly acquired image by approximately 10% towards the four corner points, using the centroid of the newly acquired image as the midpoint.

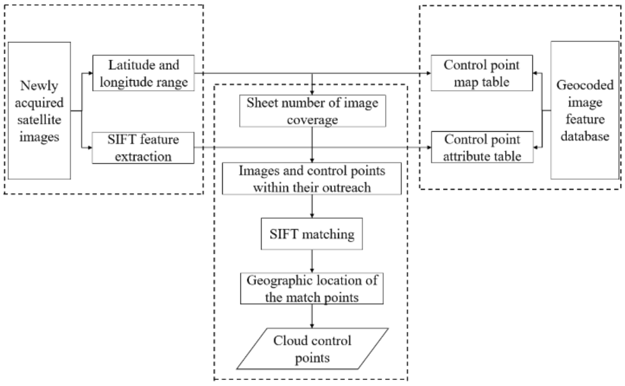

Figure 3. Workflow of matching control points from the image feature database.

Extract all control points located within the expanded geographic range of the newly acquired image, and individually match these points with the SIFT features of the newly acquired image. Assign the geographic positions of the matched feature points to the corresponding feature points in the newly acquired satellite images.

2.5 Satellite Image Orientation Based on the Geocoded Image Feature Database

The dense control points obtained from the geocoded image feature database are utilized to compensate for systematic errors of the newly acquired satellite images, thereby improving the positioning accuracies. The steps are as follows:

a) Obtain the rational polynomial coefficients (RPC) of the image, and project the acquired cloud control points onto the image using these RPC parameters to obtain projection coordinates.
b) Validate the accuracy of the cloud control points by comparing the measured coordinates of these points with their projection coordinates.
c) Utilizing cloud control points to calculate the affine transformation parameters between the measured coordinates and the projected coordinates, the systematic errors of the RPC are eliminated, thereby enhancing the accuracy of geometric positioning of satellite images.

Since there are systematic errors in the RPC, these errors determine the differences between the measured coordinates and projection coordinates of the cloud control points. Therefore, a certain number of cloud control points can be used to compensate for the systematic errors in the image space coordinates, determining correction parameters, and thus achieving high-precision georeferencing of the satellite images. By using different numbers of cloud control points for satellite image orientation and eliminating the systematic errors of RPC, it is also possible to explore the optimal number of control points for achieving high-precision geometric orientation of satellite images.

3. Experiment

3.1 Datasets

To verify the feasibility of the proposed method, the public orthophotos and SRTM DEM are used as reference data to construct the geocoded image feature library. For the geometric positioning experiments based on the geocoded image feature database, three groups of images from Tianhui-1, Ziyuan-3 and Gaofen-2 satellites are used for test. The coverage of these images encompasses two types of typical terrain: mountainous and urban areas. Table 1 describes the main parameters of the images in the experiment.

Image ID	Satellite	GSD	Acquisition Time	Area
TH01-0412S	Tianhui-1	5m	12 April 2020	3600km^2
ZY3-01a-897	Ziyuan-3	2.5m	12 August 2013	1670km^2
GF2P1-312P	Gaofen-2	0.8m	12 March 2021	516km^2

Table 1. The main parameters of the test images.

The test Tianhui-1 satellite image captured on 12 April 2020, boasts a ground sampling distance (GSD) of 5 m and covers an area of 3600 km^2. The test Ziyuan-3 satellite image with a finer GSD of 2.5 m, documents an area of 1670 km^2 on 12 August 2013. Lastly, the test Gaofen-2 satellite image, obtained on 12 March 2021, presents the highest spatial resolution at 0.8 m, encompassing an area of 516 km^2.

In the reference data, the GSDs of the public orthophotos and SRTM DEM are 2 m and 30 m, respectively. The data sizes of the corresponding DOMs for the test Tianhui-1, Ziyuan-3 and Gaofen-2 images are 6131 MB, 1568 MB and 459 MB, whereas the corresponding SRTM DEM data sizes are all about 5~10MB. The use of the high-precision reference orthophoto and DEM to obtain the three-dimensional spatial coordinates of the ground points corresponding to the feature points ensures the accuracy of the cloud control points, thus improving the geometric positioning accuracies of the newly acquired satellite images and providing a data base for the reliability and accuracy of the experiment.

In the experimental data, the width and height of the test Tianhui-1 satellite image is 12,000 pixels, and the specific location is at 36°~37°N latitude and 80°~81°W longitude, as shown in Figure 4, which is the image of the city of Winston-Salem (North Carolina, USA) and its surrounding areas.

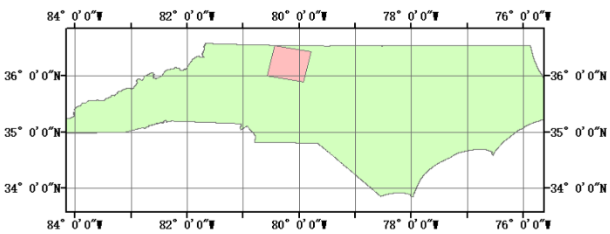

Figure 4. Footprint of the test Tianhui-1 satellite image.

The experimental Ziyuan-3 satellite image is a forward image, which has a width of 24,516 pixels and a height of 24,576 pixels and is located at latitude 30°~31°N and longitude 114°~115°E in Wuhan, Hubei Province, China, as shown in Figure 5.

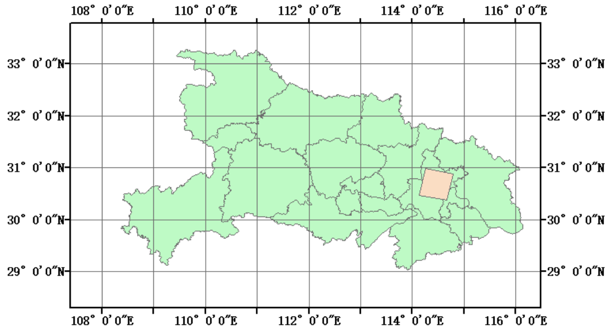

Figure 5. Footprint of the test Ziyuan-3 satellite image.

The experimental Gaofen-2 satellite image, with a width of 29,200 pixels and a height of 27,620 pixels, is located around latitude 31°N and longitude 103°E in Wenchuan, Sichuan Province, China, as shown in Figure 6.

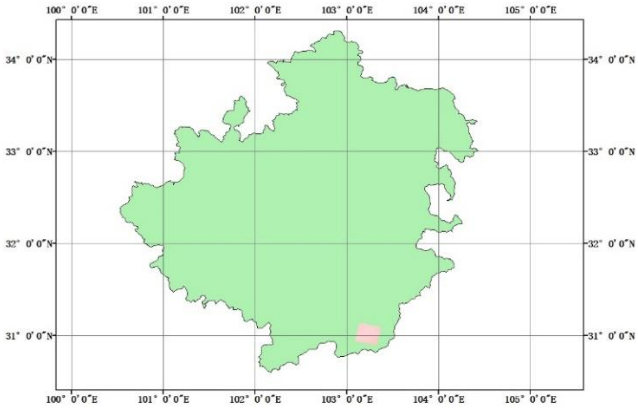

Figure 6. Footprint of the test Gaofen-2 satellite image.

Figures 7 shows the overview of the test images of Tianhui-1 satellite, Ziyuan-3 and Gaofen-2 satellites.

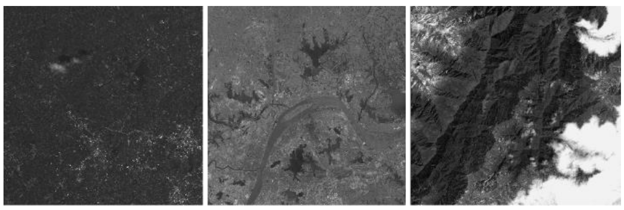

(a) (b) (c)

Figures 7. Overview of the test (a) Tianhui-1, (b) Ziyuan-3, (c) Gaofen-2 satellite images.

3.2 Results

By conducting feature extraction and geocoding on the images, the proposed method can compress DOM data of 174~1242 MB 2 m and 30 m DEM data of 6 MB into approximately 5 MB of feature point information with precise three-dimensional spatial coordinates.

By matching with the geocoded image features, a total of 372, 470, and 994 control points were obtained for Tianhui-1, Ziyuan-3, and Gaofen-2 satellite images, respectively. These points are distributed as shown in Figures 8.

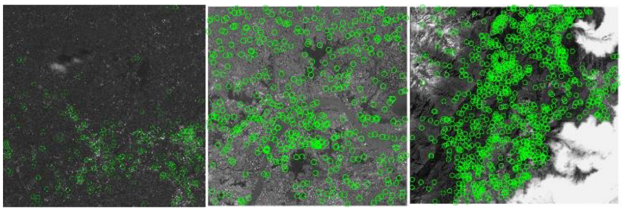

(a) (b) (c)

Figures 8. Distributions of cloud control points for (a) Tianhui-1, (b) Ziyuan-3, (c) Gaofen-2 satellite images.

When matching with the geocoded image feature database, the cloud control points obtained for satellite images are primarily distributed in urban areas with rich texture details. For large areas of vegetation, water, and other features with uniform or insufficient texture details, it is challenging to extract cloud control points. This difficulty is determined by the characteristics of SIFT feature extraction and matching.

The cloud control points are used to compensate for systematic errors in RPC to achieve high-precision positioning. Table 2 shows the accuracies of images before and after systematic error compensation.

Image ID	Before system error compensation		After system error compensation	
	σ_x	σ_y	σ_x	σ_y
TH01-0412S	2.24	2.17	1.25	1.22
ZY3-01a-897	2.67	2.55	0.86	0.67
GF2P1-312P	117.21	95.09	1.99	1.78

Table 2. Comparison of image positioning accuracies before and after system error compensation (unit: pixels)

Table 2 illustrates that the root mean square reprojection errors, specifically in the row and column directions, are diminished upon the application of systematic error compensation through cloud control points on Tianhui-1, Ziyuan-3 and Gaofen-2 satellite images. This reduction in error contributes to enhanced positioning accuracy of the satellite images. After the systematic error of RPC is eliminated by using the error compensation method in image space, the reprojection errors in the row and column directions are reduced to less than 2 pixels. This substantial improvement illustrates the correctness and applicability of the photogrammetric method of georeferencing of satellite images with geocoded image feature database.

3.3 Discussions

3.3.1 Effect of the Number of Cloud Points on the Georeferencing Accuracy

Using different numbers of cloud control points for image orientation, the residual errors of image points are expressed. The distributions of reprojection errors of image points of Tianhui-1, Ziyuan-3, and Gaofen-2 satellite images after system error compensations with different numbers of control points are shown in Figures 9, Figures 10, and Figures 11, respectively.

Figures 9, Figures 10 and Figures 11 show that there are system errors before systematic error compensation. The directions of the errors are roughly the same. This indicates that there is a certain amount of systematic error. After using a specific number of control points for systematic error compensation, the directions of the errors changes, and the error values decrease. This indicates that the method can effectively compensate for systematic errors and improve the positioning accuracies of the satellite images. As the number of control points increases, the errors gradually decrease. Utilizing all control points to compensate for system errors reduces the error values of most points.

However, some individual points still have large error values due to the incomplete elimination of coarse points during satellite image orientation. Therefore, it is necessary to improve the accuracy of feature matching and screen the acquired cloud control points before performing satellite image orientation. This will ensure the accuracy of satellite image orientation based on cloud control points.

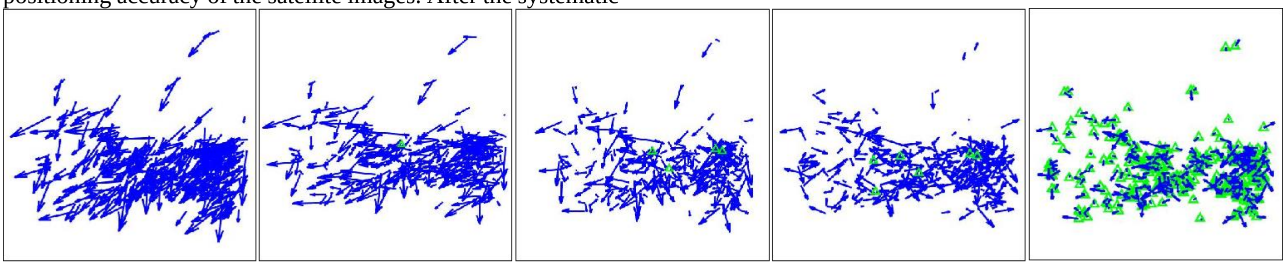

(a) (b) (c) (d) (e)

Legend: △ control points → point residual vector (1 pixel)

Figures 9. Distribution of residual errors of image points of Tianhui-1 satellite image using (a) no control point, (b) 1 control point, (c) 4 control points, (d) 6 control points, and (e) all control points for system error compensation.

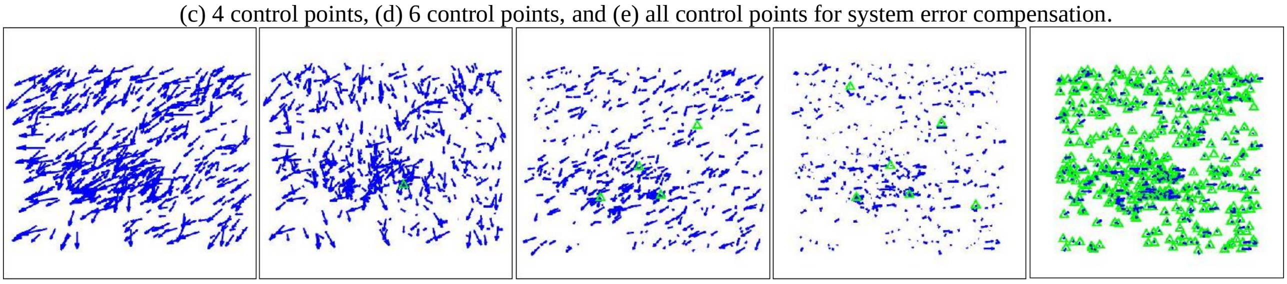

(a) (b) (c) (d) (e)

Legend: △ control points → point residual vector (1 pixel)

Figures 10. Distribution of residual errors of image points of Ziyuan-3 satellite image using (a) no control point, (b) 1 control point, (c) 4 control points, (d) 6 control points, and (e) all control points for system error compensation.

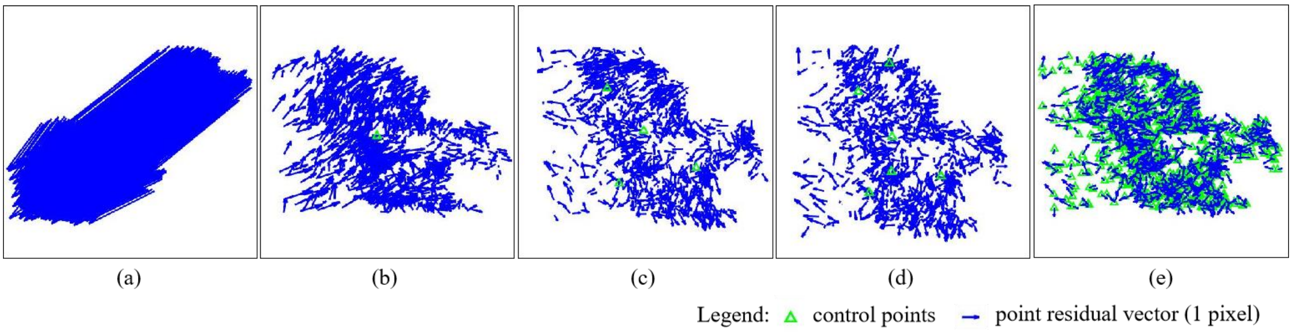

Figures 11. Distribution of residual errors of image points of Gaofen-2 satellite image using (a) no control point, (b) 1 control point, (c) 4 control points, (d) 6 control points, and (e) all control points for system error compensation.

Accuracy statistics of the above tests were performed, and the statistical results are shown in Table 3. Table 3 shows that increasing the number of control points improves the positioning accuracies of the checkpoints in both the row and column directions, as well as the overall planar positioning accuracy.

Image ID	Number of control points	Reprojection error (unit: pixel)		
		σ_x	σ_y	σ_{xy}
TH01-0412S	0	2.24	2.17	3.12
	1	1.49	1.92	2.43
	4	1.40	1.36	1.95
	6	1.26	1.34	1.84
	372	1.25	1.22	1.74
ZY3-01a-897	0	2.67	2.55	3.69
	1	1.44	2.31	2.73
	4	1.32	1.20	1.79
	6	0.99	0.90	1.34
	470	0.86	0.67	1.09
GF2P1-312P	0	117.21	95.09	150.93
	1	3.48	2.58	4.33
	4	2.37	2.02	3.11
	6	2.12	1.88	2.84
	994	1.99	1.78	2.67

Table 3. Statistics on the geopositional accuracies of satellite images using different numbers of control points

At 6 control points, the positioning accuracies of the Tianhui-1, Ziyuan-3 and Gaofen-2 satellite images in the row and column directions improve to approximately 1~2 pixels compared to those before system error compensation. However, as the number of control points increases substantially, the positioning accuracies of the checkpoints stabilize. The correlation between the number of control points and the positioning accuracies of satellite images is illustrated in Figures 12.

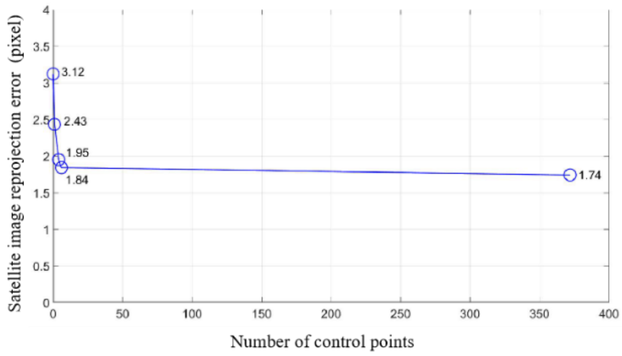

(a)

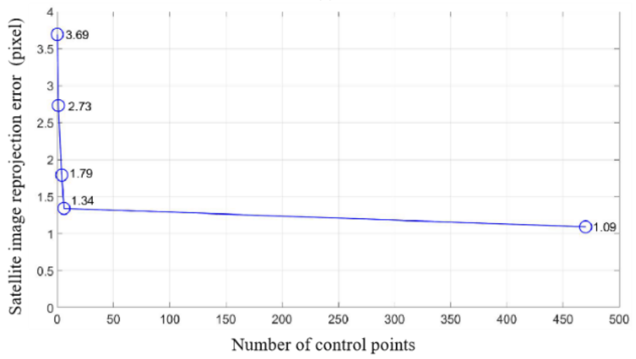

(b)

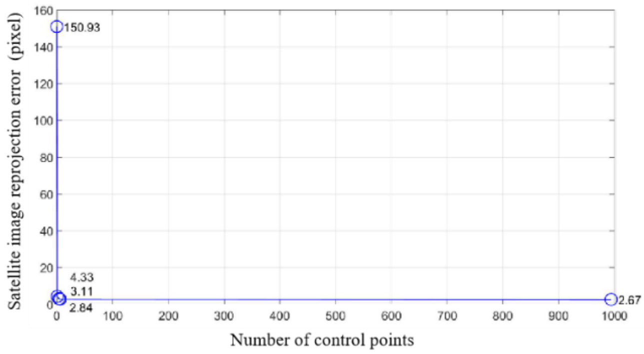

(c)

Figures 12. Relationship between the number of control points and geometric positioning accuracies of (a) Tianhui-1, (b) Ziyuan-3, (c) Gaofen-2 satellite images.

Experiments demonstrate that the direct georeferencing accuracies of the test Tianhui-1 and Ziyuan-3 satellite images are approximately 3~4 pixels, while which is approximately 150 pixels for Gaofen-2 satellite image. Following systematic error compensation, the georeferencing accuracies of the test Tianhui-1, Ziyuan-3, and Gaofen-2 satellite images improve to 1.74 pixels, 1.09 pixels, and 2.67 pixels, respectively.

3.3.2 Effect of the Resolution and Temporal Differences between Images on the GCP Matching

To explore the effect of the resolution and temporal differences between images on the GCPs obtained through matching, this paper utilizes images from three satellites captured during different periods with varying spatial resolutions, as shown in Table 1. Specifically, their respective GSDs and acquisition times are as follows: for Tianhui-1 image, 5 m in April 2020; for Ziyuan-3 image, 2.5 m in August 2013; and for Gaofen-2 image, 0.8 m in March 2021. The public orthophotos used to construct the geocoded image feature database have a GSD of 2 m, acquired in 2016.

After obtaining GCPs through matching with the geocoded image feature database and eliminating systematic errors, the positioning accuracies of all the satellite images are improved. Among them, the number of cloud control points obtained from the Gaofen-2 satellite image is the highest, leading to the most significant improvement in positional accuracy. This enhancement is primarily attributed to the superior resolution of the Gaofen-2 satellite image, which allows for the extraction of richer texture details, thus facilitating the identification of feature points for matching. Conversely, the Tianhui-1 satellite image exhibited a lower count of cloud control points due to its comparatively lower resolution and the temporal differences, potentially leading to a reduction in the number of matching points owing to variations in ground conditions.

The resolution and acquisition time of the image moderately influence the quantity of matches. Nonetheless, leveraging the geocoded image feature database proves instrumental in achieving high-precision geometric positioning of satellite images.

4. Conclusion

In addressing the issues of large data storage and slow reading efficiency associated with the DOMs and DEMs used in practical applications of cloud control based on DOM/DEM, this paper investigates a new mode of cloud control photogrammetry which uses geocoded image feature database instead of DOMs and DEMs as reference. Experimental studies were conducted on images from Tianhui-1, Ziyuan-3 and Gaofen-2 satellites. By matching with the geocoded image feature, dense cloud control points can be acquired for satellite images, thus achieving high-precision positioning of satellite images via image orientation. With the reduction of the reference data from 180~1248 MB 2 m DOM and 30 m DEM to 5~10 MB geocoded image features, the geopositional accuracies of the test Tianhui-1, Ziyuan-3 and Gaofen-2 images are improved from 3.12 pixels to 1.74 pixels, 3.69 pixels to 1.09 pixels, and 150.93 pixels to 2.67 pixels, respectively.

References

Cao H., Tao P.J., Li H.H., et al., 2019. Bundle adjustment of satellite images based on an equivalent geometric sensor model with digital elevation model. *ISPRS Journal of Photogrammetry and Remote Sensing*, 156, 169-183.

Cao, H., Tao, P.J., Li, H.H., and Zhang, Z.X., 2020. Satellite Image Positioning Method Constrained by DEM. *Acta Geodaetica et Cartographica Sinica*, 49(01), 79-91.

Chen X.W., Zhang B.M., Cen M.Y., et al., 2017. SRTM DEM-aided mapping satellite-1 image geopositioning without ground control points. *IEEE Geoscience and Remote Sensing Letters*, 14(11), 2137-2141.

Chen Y., Xie Z., Qiu Z., et al., 2015. Calibration and validation of ZY-3 optical sensors. *IEEE Transactions on Geoscience and Remote Sensing*, 53(08), 4616-4626.

LOWE, D. G., 2004. Distinctive Image Features from Scale-invariant Key Points. *International Journal of Computer Vision*, 60(2), 91-110.

Tao, P.J., Lu, L.P., Zhang, Y., Xu, B., and Zou, S.B., 2014. On-orbit Geometric Calibration of the Panchromatic/Multispectral Camera of the ZY-1 02C Satellite Based on Public Geographic Data. *Photogrammetric Engineering & Remote Sensing*, 80(06), 505-517.

Wang, H., Chen, N., and Qin, Y.G., 2021. Regional Network Adjustment Method for High-Resolution Remote Sensing Images Based on SRTM Control. *Beijing Surveying and Mapping*, 35(03), 303-307.

Xie, J.F., Ren C., Jiao H., Pan J., 2021. In-orbit geometric calibration approach and positioning accuracy analysis for the Gaofen-7 laser footprint camera. *IET Image Processing*, 15(13), 3130-3141.

Zhang G., Xu K., Jia P., et al., 2019. Integrating stereo images and laser altimeter data of the ZY3-02 satellite for improved earth topographic modeling. *Remote Sensing*, 11(20), 2453.

Zhang, H., Zhang, G., Jiang, Y.H., and Wang, T.Y., 2016. Orthorectification of Optical Satellite Remote Sensing Stereo Imagery Controlled by SRTM-DEM. *Acta Geodaetica et Cartographica Sinica*, 45(03), 326-331+378.

Zhang, Y.J., Zhang, Z.X., and Gong, J.Y., 2021. Generalized Photogrammetry of Spaceborne, Airborne, and Terrestrial Multi-Source Remote Sensing Datasets. *Acta Geodaetica et Cartographica Sinica*, 50(1), 1-11.

Zhang, Z.X., Lu, L.P., Tao, P.J., et al, 2011, November. Registration of CBERS-02B satellite imagery in quick GIS updating. In MIPPR 2011: *Remote Sensing Image Processing, Geographic Information Systems, and Other Applications* (Vol. 8006, pp. 83-90). SPIE.

Zhang, Z.X., Tao, P.J., 2017. An Overview on "Cloud Control" Photogrammetry in Big Data Era. *Acta Geodaetica et Cartographica Sinica*, 46(10), 1238-1248.

Zhang, Z.X., Duan, Y.S., Tao, P.J., 2023. From Ground Control Point to Digital Control Photo. *Geomatics and Information Science of Wuhan University*, 48(11): 1715-1723.

Zhong, B., Dai, X.Q., Cao, X.Q., and Zhang, M.H., 2019. Regional Network Adjustment Technology for Large Area Satellite Images Assisted by Control Network. *Science of Surveying and Mapping*, 44(08), 168-173.